Molecular Genetics and Metabolism 116 (2015) 178–186

Contents lists available at ScienceDirect

Molecular Genetics and Metabolism

journal homepage: www.elsevier.com/locate/ymgme

Research Article

Asparagine Synthetase Deficiency causes reduced proliferation of cells under conditions of limited asparagine

Elizabeth Emma Palmer [a,b,c,1], Jaclyn Hayner [d,1], Rani Sachdev [a,b], Michael Cardamone [a,b], Tejaswi Kandula [a,b], Paula Morris [e], Kerith-Rae Dias [e], Jiang Tao [e], David Miller [e], Ying Zhu [c], Rebecca Macintosh [a], Marcel E. Dinger [e,f], Mark J. Cowley [e,f], Michael F. Buckley [b,g], Tony Roscioli [a,b,g], Ann Bye [a,b], Michael S. Kilberg [d], Edwin P. Kirk [a,b,g,*]

[a] Sydney Children's Hospital, High Street Randwick NSW 2031, Australia
[b] University of New South Wales, High Street, Sydney, NSW 2052, Australia
[c] Genetics of Learning Disability (GOLD) service, Corner of Turton and Tinonee Roads, Waratah NSW 2298
[d] Department of Biochemistry & Molecular Biology, University of Florida College of Medicine, 1200 Newell Drive, Florida, USA, 32608
[e] Kinghorn Centre for Clinical Genomics, Garvan Institute of Medical Research, 384 Victoria Street, Darlinghurst, Sydney, NSW 2010, Australia
[f] St Vincent's Clinical School, University of New South Wales, 390 Victoria Street, Darlinghurst, Sydney, NSW 2010, Australia
[g] Seals Molecular Genetics, POW Hospital Campus, Barker Street, Randwick, Sydney, NSW 2031, Australia

ARTICLE INFO

Article history:
Received 17 May 2015
Received in revised form 10 August 2015
Accepted 11 August 2015
Available online 14 August 2015

Keywords:
Exome sequencing
Asparagine
Intellectual disability
Epileptic encephalopathy
ATP binding

ABSTRACT

Asparagine Synthetase Deficiency is a recently described cause of profound intellectual disability, marked progressive cerebral atrophy and variable seizure disorder. To date there has been limited functional data explaining the underlying pathophysiology. We report a new case with compound heterozygous mutations in the *ASNS* gene (NM_183356.3:c. [866G>C]; [1010C>T]). Both variants alter evolutionarily conserved amino acids and were predicted to be pathogenic based on *in silico* protein modelling that suggests disruption of the critical ATP binding site of the ASNS enzyme.

In patient fibroblasts, *ASNS* expression as well as protein and mRNA stability are not affected by these variants. However, there is markedly reduced proliferation of patient fibroblasts when cultured in asparagine-limited growth medium, compared to parental and wild type fibroblasts. Restricting asparagine replicates the physiology within the blood–brain-barrier, with limited transfer of dietary derived asparagine, resulting in reliance of neuronal cells on intracellular asparagine synthesis by the ASNS enzyme. These functional studies offer insight into the underlying pathophysiology of the dramatic progressive cerebral atrophy associated with Asparagine Synthetase Deficiency.

1. Introduction

Compound heterozygous or homozygous missense variants in the *ASNS* gene, encoding the enzyme asparagine synthetase, have been recently shown to cause Asparagine Synthetase (ASNS) Deficiency characterised by progressive microcephaly, cerebral atrophy and profound developmental delay. To date there are six affected families and five pathogenic variants in the *ASNS* gene reported in the literature [1–3]. Other common clinical features include intractable neonatal or infantile onset seizure disorders and axial hypotonia with appendicular hypertonia and hyperreflexia (Table 1). Some, but not all, affected individuals with ASNS deficiency have measurable abnormalities in their plasma, urine or CSF amino acids (summarised in Table 1). However, these differences, particularly in plasma and urine, can be subtle due to the differences between cerebral and peripheral asparagine metabolism and transport, and limitations of amino acid measurement [4].

The exact cause of neurological dysfunction in patients with ASNS Deficiency has not yet been fully elucidated. Here, we describe a seven year old boy with ASNS Deficiency due to novel compound heterozygous missense mutations in the *ASNS* gene. We confirm that ASNS Deficiency has a characteristic clinical and biochemical profile. We expand the current clinical literature by describing functional studies on fibroblasts from the affected individual, his unaffected heterozygous parents, and an unaffected control.

Abbreviations: AED, antiepileptic medication; AMP, adenosine monophosphate; ASNase, asparaginase; ASNS, asparagine synthetase; ATP, adenosine triphosphate; CSF, cerebral spinal fluid; DD, developmental delay; DMEM, Dulbecco's modified Eagle medium; EEG, electroencephalogram; ES, exome sequencing; GTC, generalised tonic clonic; HC, head circumference; MRI, magnetic resonance imaging; MRS, magnetic resonance spectroscopy; mTOR, mammalian target of rapamycin; NA, not applicable; NR, not reported; NT, not tested; WT, wild type.

* Corresponding author at: Department of Medical Genetics, Sydney Children's Hospital, High Street, Randwick, NSW 2031, Australia.
E-mail address: e.kirk@unsw.edu.au (E.P. Kirk).

[1] These authors contributed equally to this work.

http://dx.doi.org/10.1016/j.ymgme.2015.08.007
1096-7192/

2. Materials and methods

2.1. Exome sequencing

High quality DNA was obtained by extraction from peripheral blood in EDTA. Next Generation Sequencing was performed using a Nextera rapid capture expanded exome kit, with libraries analysed on an Illumina HiSeq2500. Reads were aligned to Human Genome Reference Sequence Hg19/GRCh37 using BWA MEM, and single nucleotide and short insertion/deletion variants were identified using HaplotypeCaller from GATK.

Data filtering and variant prioritization were performed using aligned BAM files and GEMINI (v 0.5.1b), incorporating data from dbSNP (version 138), the 1000 Genomes project (release date 21/05/2011), and the Exome Variant Server (EVS) database (ESP6500SI-V2), and Combined Annotation Dependent Depletion (CADD) database. Variants were filtered out if they were in dbSNP, had a frequency of >1% in both 1000 Genomes and EVS, were present in an in-house control, or were predicted to have a low impact on protein function. Any candidate variants from prioritization were further assessed for pathogenicity using the following *in silico* prediction tools (SIFT, PolyPhen2, PROVEAN, CADD) and were manually checked on the Binary Alignment Map files through Integrative Genomics Viewer (IGV) [5]. Informed consent for exome sequencing was obtained and the research was approved by the ethics committee from The Sydney Children's Hospital Network and the Prince of Wales Hospital Campus, Sydney, Australia (HREC ref no 13/094 and LNR/13/SCHN/112).

2.2. Sanger confirmation

To verify the candidate variants, bidirectional Sanger sequencing was performed.

2.3. Protein modelling

A model of human ASNS was generated with SWISS-MODEL using the glutamine-dependent bacterial ASNS-B structure (PDB ID 1CT9) as a template [6–10]. The model of human ASNS matched the bacterial structure well, and the adenosine monophosphate (AMP) molecule from the bacterial structure was superimposed onto the human model.

2.4. Fibroblast cell line generation and culturing

Fibroblast cell lines were generated from the patient and parents using standard methodology [11]. These primary fibroblasts as well as wild type fibroblasts from the American Type Culture Collection (ATCC) were cultured in supplemented Dulbecco's modified Eagle medium (DMEM), as described previously [12].

2.5. RNA isolation and quantitative RT-PCR

Fibroblast cells were seeded at a density of 5×10^4 per well in a 12-well plate, with three wells per condition and time point. Culture medium was changed to fresh medium 12–14 h to achieve a nutritional "basal state" before treating cells as described in the text. RNA was collected using TRIzol Reagent (Invitrogen) per the manufacturer's protocol. A 1 μg sample of total RNA was converted to cDNA using the qScript cDNA synthesis kit (Quanta Biosciences). To measure ASNS or glyceraldehyde-3-phosphate dehydrogenase (GAPDH) mRNA, RT-PCR was performed using SYBR Green (Life Technologies) and a CFX-Connect Real-Time System (Bio-Rad) following a protocol described previously [12]. Steady state mRNA was measured using the following primers: ASNS; GGCTGTGTGTTCAGAAGCT and AAGGAAGGGCTCCACTTT and GAPDH; GCCTTCCGTGTTCCTACCC and CCTCAGTGTAGCCCAAGATGC.

2.6. Protein isolation and immunoblotting

Fibroblasts were seeded at a density of 2×10^5 per 60-mm dish, with a single dish per condition and time point. Culture medium was changed 12–14 h to achieve a nutritional "basal state" before treatment. Cells were washed with PBS and lysed using 300 μL of RIPA buffer (50 mM Tris–HCl pH 7.4, 150 mM NaCl, 1 mM EDTA, 0.5% sodium deoxycholate, 0.1% SDS, and 1% triton X-100) supplemented with Pierce Protease and Phosphatase Inhibitor Mini Tablets (Thermo Scientific). Immunoblotting was performed as described previously [13]. Monoclonal anti-ASNS primary antibody [14] and anti-mouse-HRP secondary antibody (KPL) were used. Bound antibody was detected using Pierce ECL Western Blotting substrate (Life Technologies).

2.7. Cell growth and ASNase challenge

Fibroblasts were seeded at a density of 2.5×10^4 per 60-mm dish, with three dishes per time point and then treated with the indicated ASNase concentration. Culture medium was changed 12–14 h before ASNase treatment. At 0, 24, and 48 h post-treatment, cells were washed with PBS, collected by trypsin treatment and counted twice per sample using a Bright-Line haemocytometer (Sigma).

3. Results

3.1. Case report

Patient II: 1 (Fig. 2E) is the only child of non-consanguineous parents of Chinese/Brunei heritage. Both parents are of normal intelligence and have normal neurological examinations, including head circumferences. There is no contributory family history.

II: 1 was born at 37 weeks of gestation after an uncomplicated pregnancy, with normal routine antenatal scans at 12 and 20 weeks of gestation. Head circumference at birth was 32.5 cm (3–10th centile or 1 and 2 SD below the mean, WHO Child Growth Standards), length 48 cm (10–25th centile) and weight 3340 g (50th centile). Apgar scores were 8 at 1 min and 9 at 5 min. On day five of life, he was noted to have 'jittery' movements and episodic 'stiffening', without a specific diagnosis being made. He developed complex partial seizures in the first four weeks of life and an EEG showed left temporal epileptiform activity.

He was initially commenced on phenobarbitone but progressed to frequent prolonged tonic seizures which have remained resistant to polypharmacy. Other seizure phenotypes include generalised tonic clonic and multifocal clonic/myoclonic seizures. Since 2 years of age, he has had multiple daily seizures and a propensity to status epilepticus. EEGs evolved to show multifocal independent spike foci on an abnormal slow, disorganised background. Drug trials have included phenytoin, topiramate, nitrazepam, levetiracetam and sodium valproate. A reduction in seizure frequency, as measured by the number of hospitalisations for seizures (but not seizure cessation), occurred after commencement of lamotrigine.

His developmental progression was limited in the first year of life; at the age of 18 months he had some volitional hand use including the ability to transfer and throw objects. Subsequently, there has been developmental regression and stagnation: aged eight, he has no volitional hand function, is wheelchair bound, fully dependent for all activities of daily living, fed *via* PEG tube and has profound intellectual disability and cortical visual impairment. He has no evidence of a sensorineural hearing deficit and has a structurally normal ophthalmological examination.

On examination at age 6 he had postnatal microcephaly (see head circumference chart Fig. 1C), sloping forehead with relatively prominent midface, axial hypotonia with significant head lag and an inability to sustain a sitting position. He had appendicular hypertonia with limb hyperreflexia, clonus and up-going plantars.

Table 1
Comparison of Phenotype and Genotype for reported patients with Asparagine Synthetase Deficiency compared to affected patient described in this report.

Family (Ref)	Compound heterozygous/homozygous Patient (s) Ethnicity	Nucleotide change	ASNS modification	Frequency of variant in EXAC database (accessed March 2015)	Position of variant in protein model	1.Grantham Score 2. Polyphen-2 3. SIFT 4. PROVEAN	ASNS protein levels in transfected cells	ASNS protein levels in patient fibroblasts	Effect of asparaginase on cellular proliferation
Family 1 (this patient)	Compound heterozygote Chinese/ Brunei	c.866G>C	p.Gly289Ala	NR but p.Gly289**Asp** reported with allele frequency 8.243e-06 (1 heterozygote/ 121316 tested individuals)	In the C-terminal asparagine synthase domain near ATP binding pocket	1.60 2.Probably damaging (0.908) 3.Damaging (0.000) 4.Deleterious (-6)	N/A	Unchanged compared to wild type or heterozygous parents. N.B. *ASNS* expression increased when fibroblasts cells depleted of asparagine by adding asparaginase.	Reduced cellular proliferation in patient fibroblasts compared to heterozygous parents and WT
		c.1010C>T	p.Thr337Ile	NR	In the C-terminal asparagine synthase domain near ATP binding pocket	1.89 2.Probably damaging (1) 3.Damaging (0.002) 4.Deleterious (-5.13)	N/A		
Family 2 (Ruzzo et al family A: 1 male patient)	Homozygous Iranian Jews	c.1084T>G	p.Phe362Val	NR but n.b. another missense at that location. reported with allele frequency 8.282 x 10^{-6} (1 heterozygote/ **120748** tested individuals)	In the C-terminal asparagine synthase domain	1.50 2.Damaging (0.95) 3.Damaging (0.04) 4.Deleterious (-6.49)	Reduction in protein abundance	One patient (II.1 from family A) reduced ASNS abundance	NT
Family 3 (Ruzzo et al family B: male and female siblings)	Homozygous Iranian Jews								
Family 3 (Ruzzo et al family C: 3 male patients)	Homozygous Bangladeshi	c.1648C>T	p.Arg550Cys	p.Arg550Cys 2 heterozygouts / 121,182 tested individuals or allele frequency 1.65^{-5}	R550 is located in the C terminal region of the ASNS protein and the exact location in the protein can not be resolved as crystallographyof distal c terminal region not available.	1.180 2.Damaging (1) 3.Damaging (0.01). 4.Deleterious (-6.49)	Increase in protein abundance	NT	NT
Family 4 (Ruzzo et al family D: 3 male patients)	Compound heterozygous French Canadian	c.1648C>T	p.Arg550Cys	p.Arg550Cys 2 heterozygouts / 121182 tested individuals or allele frequency 1.65-$^{05.2}$	R550 is located in the distal C terminal region of the ASNS protein.	1.180 2.Damaging (1) 3.Damaging (0.01) 4.Deleterious (-6.49)	Increase in protein abundance	NT	NT
		c.17C>A	p.Ala6Glu	p.Ala6Val 2 heterozygotes out of 120,784 individuals. Allele frequency 1.65 x 10^{-5}	In the N-terminal glutamine aminotransferase domain	1.107 2.Damaging (0.898) 3.Damaging (0.02) 4. Deleterious (-3.55)	Reduction in protein abundance	NT	NT
Family 5 (Ben Salem et alL: one affected male)	Homozygous Emirati	c.1193A>C	p.Tyr398Cys	**p**.Tyr398Cys reported in 1 heterozygote/ 121206test individuals Allele frequency 8.25 x 10^{-6}	In the C-terminal asparagine synthase domain near beta aspartyl AMP intermediate formation site	1.194 2. Probably damaging 3. Damaging (0.01) 4. Deleterious (-8)	NT	NT	NT
Family 6 (Alfadhel et al: male and female siblings)	Homozygous Saudi Arabian	c.1130A>G homozygous [n.b. non canonical transcript NM_001178075.1 personal communication Alfadhel, 2015)	p.Tyr377Cys	NR	In the C-terminal asparagine synthase domain	1.194 2. Probably damaging (1) 3. Damaging (0.001)(g) 4. Deleterious (-8.19)	NT	NT	NT

Family (Ref)	Neurological phenotype	Epilepsy phenotype including EEG	Neuroimaging/ Neuropathology in case of post mortem	Plasma amino acids
Family 1 (this patient)	-Head circumference 32 cm at birth -Progressive postnatal microcephaly. -Profound DD with developmental regression at 18 months. Maximum developmental age ~6/12. -Cortical blindness -Profound axial hypotonia and appendicular hypertonia and hyperreflexia. -Worsening of movement disorder with phenytoin infusions.	-Jittery episodes and episode of 'stiffening' noted day 5 life -Onset seizures within first 4 weeks of life Type of seizures: mainly tonic (occ status) and occasional complex partial. -Variable EEGs mainly multifocal epileptogenic foci with abnormal background. -Seizure treatment: intractable to polytherapy and worsening with age. Some seizure reduction with lamotrigine.	- **MRI** 3 months: structurally normal other than microcephaly.**-MRI- 4 years**. Progressive cortical and subcortical atrophy with moderate generalised enlargement of the ventricular system and diffusely thin corpus callosum. Slender brainstem. Cerebellum not affected.No simplified gyri **MRS** non-diagnostic but showing lactate peak	Glycine raised 472 umol/L (normal 119–368); Asparagine low 18(22–81) Phenylalanine low (27) 30–75. (parents never consented for CSF amino acids).
Family 2(Ruzzo et al. family A: 1 male patient) Family 3 (Ruzzo et al. family B: male and female siblings)	-Head circumference 31–31.5cm at birth -Progressive postnatal microcephaly -Profound DD -Cortical blindness -No axial hypotonia but appendicular hypertonia and hyperreflexia. -No hyperekplexia	-Jittery episodes from birth with episode of spasticity -Seizure onset 2 weeks to 1 month -Type of seizures: infantile spasms, evolving to tonic and myoclonic seizures. -EEG: hysparrythmia evolving to multiple independent spike foci on slow background -Seizure treatment: tonic and myoclonic seizures partially responsive to AED polytherapy.	**MRI 3 months-** diffuse cerebral atrophy, enlarged- extra-ventricular spaces with normal size cerebellum and brainstem **MRI by 18 months**, progressive cortical and subcortical atrophy with delayed myelination, moderately enlarged lateral ventricles and thin corpus callosum. Small brain stem with only very mildly affected cerebellum. -Pons size not decreased -No simplified gyri	Not available (family A) Family B Glutamine raised (2/2) Asparagine and aspartate normal (2/2)
Family 3 (Ruzzo et al. family C: 3 male patients)	-HC at birth 30.5cm- 33cm -Progressive postnatal microcephaly -Profound DD -Cortical blindness -Axial hypotonia 2/3 -Appendicular hypertonia (3/3) -Died between 3 and 6 months of age of aspiration pneumonia -Episodes of hypothermia	-Jittery episodes and hyperekplexia from birth -No seizures -EEG: disorganised background	**MRI**: decreased cerebral volume -Decreased size of pons -Simplified gyri -1st sibling: Initial MRI showed left transverse sinus thrombosis and cerebral dysgenesis -2nd sibling mild restricted diffusion of both thalami and ?basal ganglia **MRS** mildly elevated lactate peak.	Aspartate low (1/1) Asparagine low (1/1)
Family 4 (Ruzzo et al. family D: 3 male patients)	-HC at birth 28.5cm (at 33.5 weeks gestation) to 31.5cm -Progressive postnatal microcephaly -Profound DD -Axial hypotonia -Appendicular hypertonia -Episodes of hypothermia - Died between 4 days and 12 months of age of aspiration pneumonia.	-Onset seizures 4 days to 9 months. Patient with later seizure onset had tremulous movements and abnormal EEG at 4 days. -Type of seizures: tonic, orobuccal, partial complex. -EEG suppression bursts and MISF. -Partial seizures controlled with monotherapy AED	**MRI**-decreased cerebral volume -Decreased size of pons -Simplified Gyri **Post mortem findings** 1st sibling: cortical dysgenesis, absence of the bulbar arcuate nucleus, periventricular leukomalacia; and marked gliosis. 2nd sibling: severe mesial temporal sclerosis and neuronal loss in regions CA3, CA4 and CA1, dysplasia of the olivary nucleus. Hydromelia of the spinal cord with secondary degeneration of motor neurons and reactive gliosis.	Glutamine low (1/2) and normal (1/2) Aspartate normal (2/2) Asparagine low (1/2) and normal (1/2)
Family 5 (Ben Salem et alL: one affected male)	-HC at birth 29.5cm -Progressive postnatal microcephaly -Profound DD -Cortical blindness -Axial hypotonia -Appendicular hypertonicity and hyperreflexia	-Seizure onset first day life -Type :Myoclonic -EEG: multiple independent spike foci. -Treatment: intractable to polytherapy with AED	**MRI**- Severe microcephaly -Ventriculomegaly -Decreased size of pons -Thin corpus callosum -Simplified gyral pattern	Normal plasma and urine amino acids
Family 6 (Alfadhel et al.: male and female siblings)	HC at birth 26.5cm- 30cm Progressive postnatal microcephaly Profound DD Axial hypotonia Appendicular hypertonicity and hyperreflexia	-Seizure onset on first day of life -Type: GTC and myoclonic -EEG: multiple independent spike foci. -Treatment: intractable to polytherapy with AED	**MRI**-Severe microcephaly, brain atrophy and delayed mylination, simplified gyriform pattern	Normal plasma glutamine, high-normal csf glutamine Plasma asparagine level low, csf asparagine low (not detected),

Abbreviations: AED = antiepileptic medication; CSF = cerebral spinal fluid; EEG = electroencephalogram; GTC = generalised tonic clonic; HC = head circumference; DD = developmental delay; MISF = multiple independent spike foci; MRI: magnetic resonance imaging; MRS: magnetic resonance spectroscopy; NA = not applicable; NR = not reported; NT = not tested; WT = wild type.

He has had extensive non-diagnostic neurological/neuroradiological and metabolic investigations prior to enrolment in an exome sequencing (ES) study. He has no evidence of systemic organ involvement with normal full blood count, renal and hepatic function and normal renal ultrasounds. Serial MRI scans have demonstrated progressive generalised cerebral atrophy including atrophy of the deep grey matter in the basal ganglia. His brain MRI at 4 years (Fig. 1) demonstrated generalised cerebral atrophy of the supratentorial and infratentorial structures, thin corpus callosum, slender pons and marked reduction of white matter. Brain magnetic resonance spectroscopy (MRS) demonstrated an elevated lactate duplex at 1.3 parts per million (ppm).

3.2. Exome sequencing

Following filtering, two non-synonymous variants in *ASNS* were identified. The first is predicted to result in the heterozygous substitution of the normally encoded glycine at position 289 by an alanine. The second is predicted to result in the heterozygous substitution of the normally encoded threonine at position 337 by an isoleucine (NM_183356.3:c. [866G>C]; [1010C>T]; NP_899199.2:p. [Gly289Alal]; [Thr337Ile]). Both variants were predicted to be pathogenic using Align GVD, Polyphen-2. PhyloP, SIFT, PROVEAN and CADD (CADD scores 24.8 and 20.9 respectively). There were no other plausible candidate variants identified on ES.

3.3. Sanger sequencing

The variants were shown to be *in trans* based on bidirectional Sanger sequencing of parental samples; the mother was heterozygous for c.1010C>T and the father was heterozygous for c.886G>C (Fig. 2E).

3.4. Position of mutations in human ASNS protein

Modelling of the position of the proband's two *ASNS* variants (Fig. 2F) indicates that G289 and T337 are located near the ATP binding pocket. Therefore mutations at these sites could potentially alter ATP binding or hydrolysis reducing enzyme efficiency.

3.5. Regulation of the ASNS gene and ASNS mRNA stability are unaffected by the mutations (Fig. 3A)

Histidine deprivation of mammalian cells and tissues induces cell stress and results in transcriptional *ASNS* mRNA induction triggered by the well-characterized amino acid response (AAR) pathway [15,16]. Consequently, activating the AAR shows the functionality of *ASNS* gene regulation. Fibroblasts harbouring both pathogenic variants (affected child) did not show an increase in “basal” (with histidine) ASNS mRNA expression relative to WT or heterozygous parental cells (unaffected mother and unaffected father) (Fig. 3A). Therefore, in non-stressed conditions, mRNA expression and stability appear to be unaffected in the proband's cells. The kinetics and levels of mRNA after activation of transcription by the AAR were also similar for all cell lines suggesting that neither the heterozygous or compound heterozygous state affects the regulation of the *ASNS* gene or the stability of *ASNS* mRNA. Therefore, the clinical phenotype is not caused by reduced *ASNS* gene expression.

3.6. ASNS protein stability

ASNS protein levels were measured in fibroblast cells transferred to fresh DMEM and then monitored over a 24 h period to determine if the mutations in the proband's cells affect protein stability (Fig. 3B). ASNS protein levels were not dramatically altered in the patient's fibroblasts relative to the WT and parental cell lines indicating that the mutations do not cause aberrant degradation of the protein. Collectively, the data support the hypothesis that the mutations do not alter mRNA or protein content, but rather alter enzyme activity.

3.7. Cells harbouring both ASNS mutations do not proliferate in medium depleted of asparagine

To determine if the detected mutations affect ASNS enzymatic activity, cells were grown in culture medium depleted of asparagine by the addition of asparaginase (ASNase) to the medium. If the mutations negatively affect ASNS activity, then the patient's fibroblasts will not be able to synthesize the required asparagine, leading to slower proliferation of the patient's cells relative to that of the parental or WT fibroblasts. Fig. 3C shows that in asparagine-depleted medium, the growth of the patient's fibroblasts stagnated relative to the parental and WT fibroblasts, indicating that the detected ASNS variants deleteriously affect the asparagine synthetic function of the enzyme. The parental fibroblasts showed a slight growth defect in the highest ASNase concentration, but were still able to grow, presumably because they have one copy of a functioning enzyme and therefore, can still produce sufficient amounts of functional ASNS protein.

3.8. The stress of asparagine depletion causes increased ASNS expression in cells harbouring ASNS mutations

Even though the patient's cells did not proliferate in the ASNase treated medium, the histidine depletion experiments (Fig. 3A) indicated that transcriptional regulation of the gene was intact. To determine if asparagine depletion also activated the gene *via* the AAR, as it should, mRNA content was measured after ASNase treatment (Fig. 3D). The data showed that the proband's cells induce ASNS mRNA levels in an attempt to overcome the stress of asparagine depletion. This result was in contrast to WT fibroblasts, for which ASNS expression was unaltered, as they can synthesize enough asparagine from existing ASNS protein in asparagine-depleted conditions. As was the case for proliferation, the parental fibroblasts showed an intermediate effect with slight induction of ASNS mRNA when asparagine was depleted.

4. Discussion

Asparagine is ubiquitously required for cellular growth and function. It is considered a ‘non-essential’ amino acid, as it can be generated intracellularly from the amino acids glutamine and aspartate *via* the ATP-dependent synthetic enzyme ASNS. ASNS is composed of two distinct domains, each with a separate catalytic site (Fig. 2D). The N-terminal domain catalyzes glutamine hydrolysis to yield glutamate and ammonia. The C-terminal active site of ASNS catalyzes the ATP-dependent activation of the side-chain carboxylate of aspartate to form an electrophilic intermediate, β-aspartyl-AMP and inorganic pyrophosphate [4]. Transfer of ammonia to the aspartyl backbone completes the reaction.

We confirm characteristic neurological symptoms and signs for the diagnosis of ASNS Deficiency (Table 1). The key neurological finding is markedly progressive cerebral atrophy. Our patient's head circumference at birth was within the low normal range, as was the case for several other families (see Table 1). He had marked progressive postnatal microcephaly (Fig. 1C) which is a characteristic feature of this condition (Table 1). Although our patient had very limited developmental progress in the first year of life, he subsequently lost developmental milestones to a level of profound developmental delay, in keeping with the other reported patients. Not all other reported patients have detailed clinical information available so we do not know if developmental regression was present in other affected individuals. Other uniform neurological findings shared by our patient and the other reported individuals are axial hypotonia, appendicular spasticity and profound developmental delay [Table 1]. The lack of non-neurological symptoms may seem, at first sight, surprising given the ubiquity of ASNS protein expression and the asparagine requirement of all cells

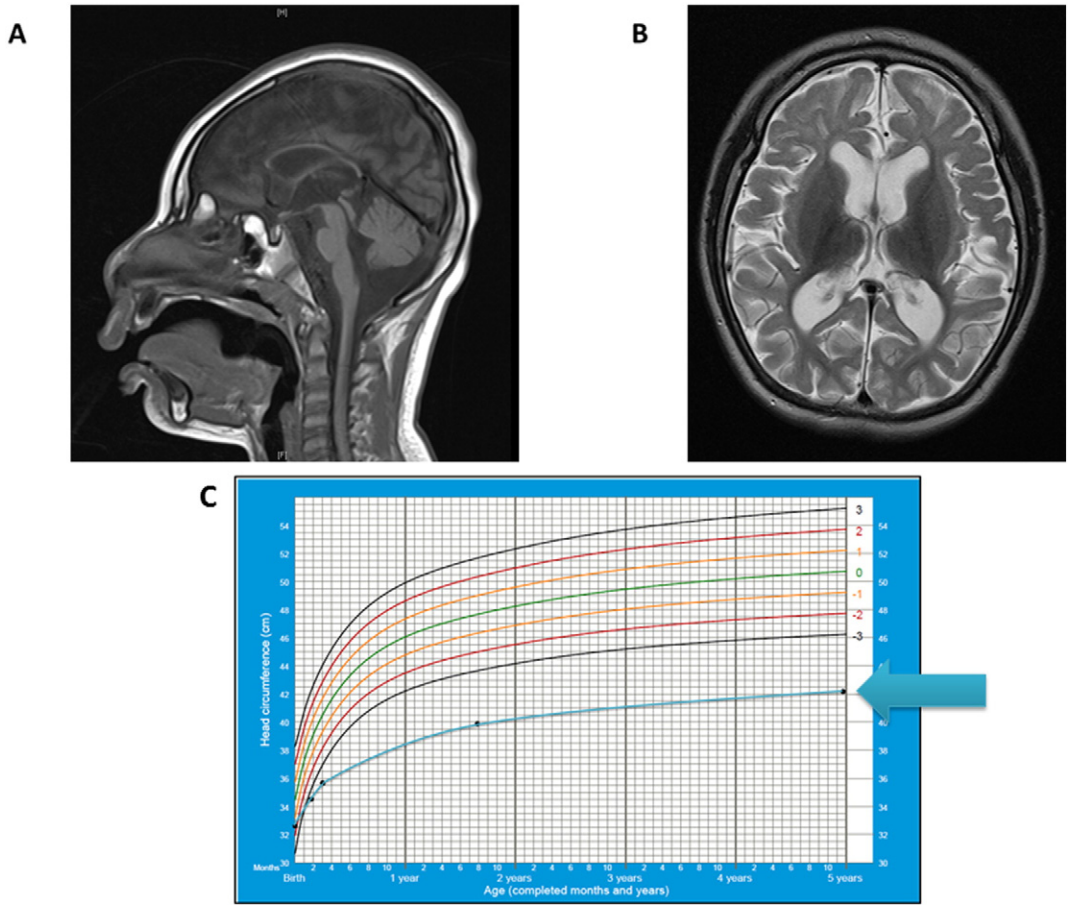

Fig. 1. A and B: MRI scan images of the proband's brain aged 4 years. A. Sagittal T1 (A) and axial T2 (B) weighted images. Note small cranial vault with craniofacial dysmorphism in keeping with microcephaly, enlargement of the ventricles (E) and the supratentorial (A) and infratentorial (B) extra-axial spaces in keeping with global atrophy in both the supratentorial and infratentorial compartments. Diffusely thin corpus callosum (C) and slender brainstem (D). C: Head circumference of proband plotted on WHO Child Growth Standard chart (http://www.who.int/childgrowth/en/ accessed July 2015) demonstrating the head circumference was between −1 and −2 SD from the mean at birth but rapidly decelerated to be below −5 SD from the mean by the age of 20 months.

for proliferation and function [4]. However, this CNS-limited effect can be explained by the ability of peripheral cells to compensate for ASNS hypo-function by utilising dietary derived asparagine. In contrast, transport of asparagine across the blood–brain-barrier is limited and reliant on transporters that also transfer other amino acids [4]. The CSF content of asparagine is 1–10% that of plasma [17]. Hence, cells within the blood–brain barrier are relatively depleted of exogenous asparagine, and dependent on intracellular ASNS synthesis. Moreover, neuronal cells have a significant requirement for asparagine in the developing and mature brain and *ASNS* is highly expressed in the human brain [4]. In embryonic mice, *ASNS* expression is concentrated within neural progenitor cells in ventricular and subventricular zones [18] pointing towards the importance of asparagine metabolism in brain development.

How the previously reported *ASNS* missense variants (1–3) result in ASNS enzymatic hypo-function had not yet been comprehensively explained. The five variants have all been non-synonymous missense variants affecting highly conserved amino acids (p.F362V; p.R550C; p.A6E; p.Y398 and p.Y377C). All have been predicted to be pathogenic based on *in silico* prediction software (Table 1) and segregated with the condition in the families.

Fibroblasts from our patient had no significant reduction in ASNS mRNA or protein levels, suggesting that the variants reported here do not decrease mRNA or protein stability or cause protein misfolding leading to the degradation of ASNS. Ruzzo et al. [1] investigated the functional effect of the p.F363V, p.A6E and p.R550C variants by producing transfected cells (HEK293) which demonstrated no alteration in ASNS mRNA level (similar to our findings), but reduced protein abundance for two variants and increased protein abundance for one variant. Despite the variability in protein expression in transfected cells, Ruzzo et al. postulated that the clinical similarity in presentation between all affected individuals point to all of the variants causing a loss of function of the ASNS enzyme. No functional studies have been published on the p.Y398 [2] and p.Y377C [3] variants. There appears to be no clear correlation between phenotypic severity and effect of ASNS mutations on protein expression (Table 1). This is more supportive of pathogenic mutations in ASNS causing pathophysiology by altering enzymatic activity rather than by reducing cellular enzyme levels. It is likely that homozygous nonsense mutations in ASNS would not be compatible with life.

Our study is novel in that we were able to demonstrate reduction in synthetic function of the Asparagine Synthetase enzyme in our patient's fibroblasts. This was demonstrated by limitation in cellular growth when the cells were depleted of asparagine by the addition of ASNase to the culture medium. We hypothesise that this limitation in asparagine replicates the situation within the blood–brain barrier, where central nervous system cells have high requirements for asparagine but have limited availability of dietary derived asparagine. This would therefore explain the selective and marked cerebral atrophy in ASNS Deficiency patients. Protein modelling of the position of the mutated

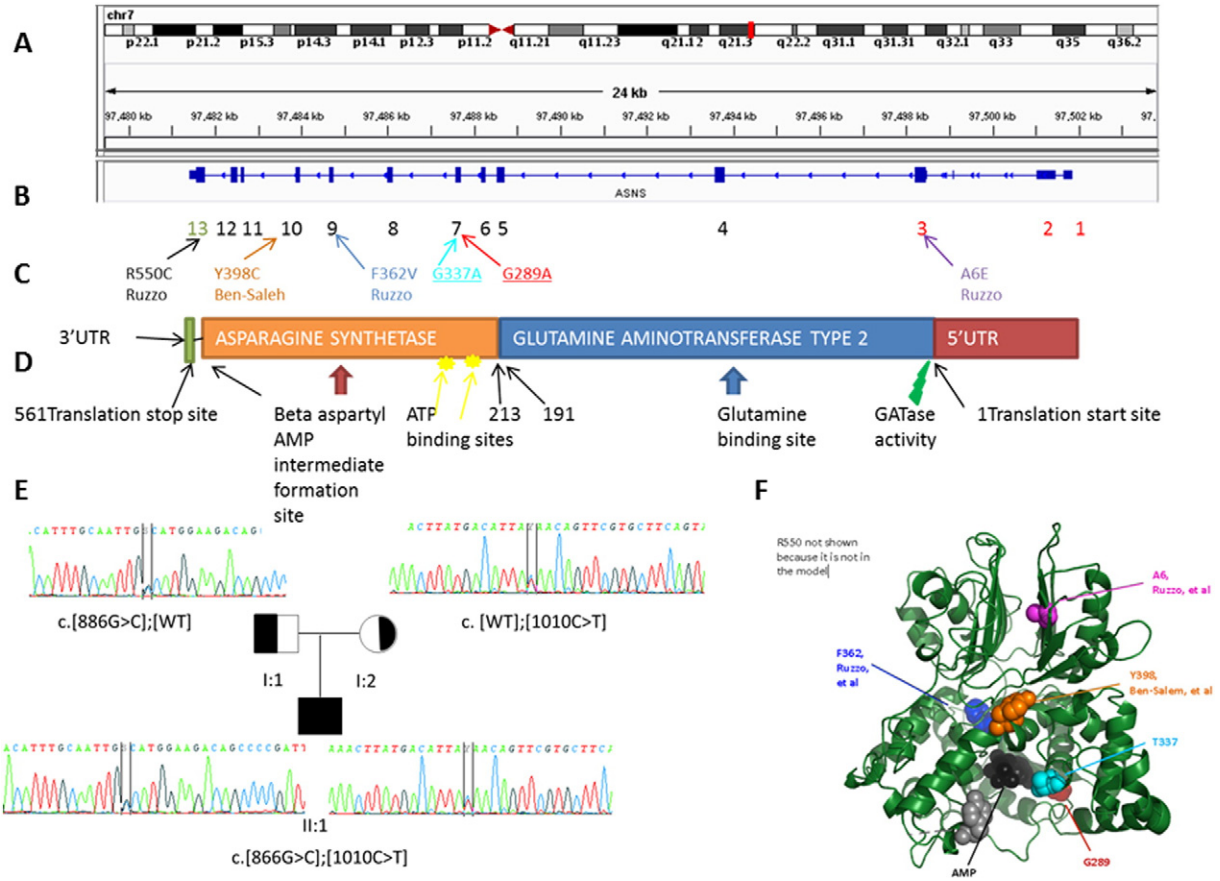

Fig. 2. A: Chromosomal location of *ASNS* at 7q21.3. B: Exons of *ASNS* gene. C: Position of G337 and G289 (this patient) in the *ASNS* gene, as well as positions of pathogenic variants described in Ruzzo et al. and Ben Saleh et al. (ref. [1,2]). Variants described are spread throughout the gene in exons 3, 7, 9, 10 and 13. The variant reported by Alfadhel et al. (ref. [3] and personal communication, Alfadhel, 2015) was not in the canonical transcript but in a shorter transcript of *ASNS* (NM_001178075.1), and therefore could not be included in this diagram. D: Functional regions of the ASNS protein (adapted from Ben Saleh et al., ref. [2]). T337 and G289 (this patient) are located proximal to the ATP binding sites that make up the ATP binding pocket. E: Pedigree and chromatograms of DNA sequence changes in the *ASNS* gene. Compound heterozygous mutations were detected in the affected child (II: 1) NM_183356.3:c.[866G>C]; [1010C>T]. His father (I: 1) is a heterozygote carrier of the c.866G>C variant and his mother (II: 2) is a heterozygote carrier of the c.1010C>T variant. F: A model of human ASNS, generated with SWISS-MODEL using the glutamine-dependent bacterial ASNS-B protein as a template (8), demonstrating the location of the variants in the proband and pathogenic variants described in Ruzzo et al. and Ben Saleh et al. (ref. [1,2]). Modelling of the position of the proband's two *ASNS* variants indicates that G289 and T337 are located near the ATP binding pocket and therefore mutations at these sites could potentially alter ATP binding or hydrolysis reducing enzyme efficiency. The R550 variant described in Ruzzo et al., (1) is not included as crystallography could not be determined for the distal end of the C-terminal region and the variant described by Alfadhel et al. (3) is not included as is in a shorter, non-canonical transcript.

amino acid residues in our patient (Fig. 2F) demonstrated that the altered residues (G289 and T337) are proximal to the ATP binding pocket and therefore mutations at these sites could potentially alter ATP binding or hydrolysis to cause reduced enzyme efficiency.

Ruzzo et al. postulated that dietary asparagine supplementation may provide therapeutic benefit in ASNS Deficiency patients, drawing on some promising effects of serine supplementation (when given prior to development of significant neurological symptoms) for the juvenile form of serine deficiency [19]. However, there are several likely barriers to the success of asparagine supplementation. As all patients described to date with ASNS Deficiency have had a small head circumference at birth and early (neonatal to early infancy) evidence of neurological dysfunction, prenatal treatment would be required. We note that serine supplementation has not had sustained therapeutic benefit when given to serine deficient patients who are already symptomatic [15]. Secondly, given the kinetics of asparagine transportation across the blood–brain barrier it is not clear that dietary supplementation of asparagine would result in significantly increased asparagine levels within the central nervous system [17]. Thirdly, the need to supplement the diet with high levels of asparagine may have detrimental effects on the uptake of other amino acids that share the same transporters [17]. This competitive effect could result in detrimental metabolic perturbation within many organs and, in particular, worsening of neurological function by limitation of other essential amino acids.

There may be additional pathophysiological effects of reduced ASNS function, such as toxicity due to the accumulation of asparagine precursors aspartic acid and glutamine. ASNS has as yet incompletely understood roles in the Glutamine–Glutamate Cycle that exists between neurons and glial cells [20]. The only ASNS Deficiency patients with documented CSF amino acids [3] did have high-normal levels of CSF glutamine (Table 1). Our patient's parents declined CSF amino acid measurement of the proband. Glutamine is a precursor to glutamate, which is a well-recognised excitotoxin and epileptogenic amino acid [21]. Therefore, such toxic effects may at least partially explain the severe epileptic phenotype demonstrated in the majority of patients.

Other avenues for therapy may include utilising antiepileptic medication that target the glutamate system, or trialling glutamate scavengers, nitric oxide inhibitors or free radical scavengers [22]. It is interesting to note that the only anti-epileptic with some possible beneficial effect in our patient was lamotrigine; this drug inhibits presynaptic voltage-gated sodium channels and reduces the presynaptic release of glutamate [23].

Mitochondrial dysfunction is thought to be important in the hepatotoxic side-effects of ASNase [24], which depletes cellular asparagine in peripheral cells by depleting plasma asparagine, leading to efflux of intracellular asparagine and then destruction in the plasma. Therefore, it would also be interesting to explore whether there is evidence of central nervous system mitochondrial dysfunction in ASNS Deficiency

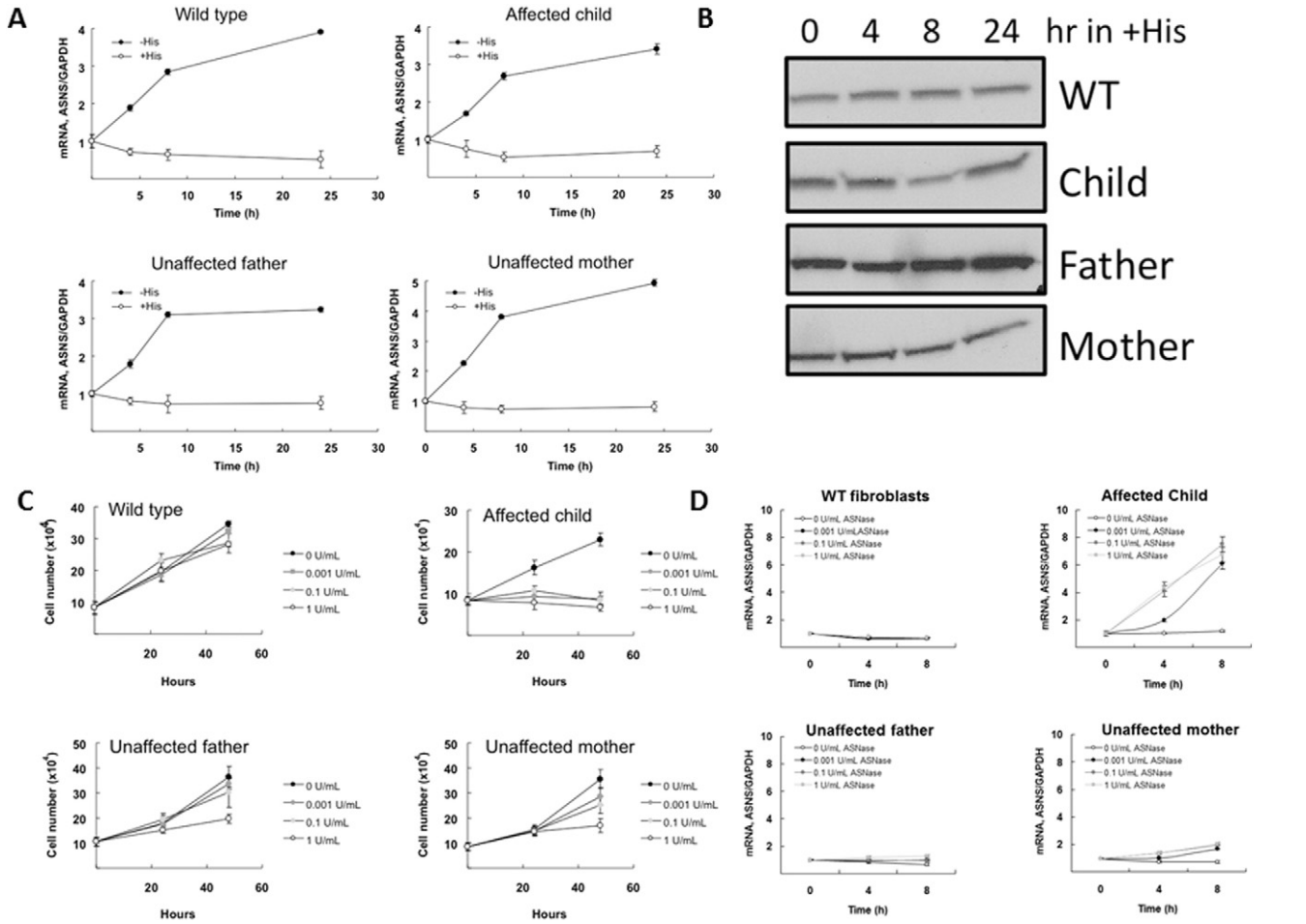

Fig. 3. A: Regulation of the *ASNS* gene and *ASNS* mRNA stability are unaffected by the mutations. To assess *ASNS* mRNA expression and stability, fibroblasts were cultured in either complete DMEM medium (+His) or DMEM lacking histidine (−His) to activate the AAR and induced mRNA expression. Cells were collected 0, 4, 8, and 24 h post-treatment and mRNA was measured by qPCR. GAPDH mRNA, which is unaffected by histidine deprivation, was used as an internal control. Averages ± standard deviation are shown. B: ASNS protein stability in fibroblast cells is unaffected by the mutations. Fibroblasts were cultured in complete DMEM for 0, 4, 8, and 24 h. ASNS protein levels were assessed by immunoblotting. C: Cells harbouring both ASNS mutations (affected child) do not proliferate in medium depleted of asparagine. Fibroblasts were cultured in DMEM containing with 0, 0.001, 0.1, or 1 U/mL of asparaginase (ASNase). At 0, 24, and 48 h post-treatment, fibroblasts were collected by trypsin treatment and counted. Cells were grown in triplicate for each ASNase concentration and time point. Averages ± standard deviation are shown. D The stress of asparagine depletion causes an increase in ASNS expression in cells harbouring ASNS mutations. Cells were cultured in DMEM containing 0, 0.001, 0.1, and 1 U/mL ASNase. Cells were collected at 0, 4, and 8 h post-treatment and steady state ASNS mRNA was measured by qPCR. GAPDH mRNA was used as an internal control, and averages ± standard deviation are shown.

patients. ASNase related hepatotoxicity has been successfully treated with mitochondrial cofactors [25]. Further insight into the possibility of CNS mitochondrial dysfunction in ASNS Deficiency patients might be obtained by monitoring with magnetic resonance spectroscopy (MRS) and CSF lactate measurement in cerebrospinal fluid (CSF) over the progress of the condition, including during exacerbations of seizures, for example with inter-current illnesses.

Our patient's brain MRS at 4 years demonstrated an elevated lactate duplex at 1.3 parts per million (ppm). He has worsening of seizure control with febrile illnesses. CSF lactate and repeat MRS studies have been declined by his parents. We note a mild lactate peak in one other patient with ASNS Deficiency who had an MRS reported (1: family C; Supplementary data and Table 1). However, there is a current lack of effective treatments for patients with a primary central nervous system mitochondrial condition, although this is an area of active research [26].

Lastly we note that asparagine metabolism and transport may be linked to the mTOR pathway [27] and targeting of this pathway, as has been successful in other mTOR related epileptogenic conditions [28] may have some benefit.

5. Conclusions

This study demonstrates how exome sequencing can alter the interpretation of previous metabolic screening in the context of careful clinical evaluation. Novel functional work on our patient's fibroblasts confirmed the pathogenicity of the novel variants, allowing accurate genetic counselling for the family. In addition, it led to new insights into the underlying pathophysiology of ASNS Deficiency and raises the possibility of targeted treatments for this devastating condition.

Acknowledgements

We thank to the patient and his family for their participation in this study. We thank to members of the Molecular Genetics and Cytogenetics teams at SEALS laboratory in particular Corrina Walsh, Glenda Mullan and Toni Saville for assistance with processing of samples. This research was supported by grants to MSK from the Institute of Diabetes, Digestive and Kidney Diseases, National Institutes of Health (DK92062 and DK94729).

References

[1] E.K. Ruzzo, J.M. Capo-Chichi, B. Ben-Zeev, D. Chitayat, H. Mao, A.L. Pappas, Y. Hitomi, Y.F. Lu, X. Yao, F.F. Hamdan, K. Pelak, H. Reznik-Wolf, I. Bar-Joseph, D. Oz-Levi, D. Lev, T. Lerman-Sagie, E. Leshinsky-Silver, Y. Anikster, E. Ben-Asher, T. Olender, L. Colleaux, J.C. Décarie, S. Blaser, B. Banwell, R.B. Joshi, X.P. He, L. Patry, R.J. Silver, S. Dobrzeniecka, M.S. Islam, A. Hasnat, M.E. Samuels, D.K. Aryal, R.M. Rodriguiz, Y.H. Jiang, W.C. Wetsel, J.O. McNamara, G.A. Rouleau, D.L. Silver, D. Lancet, E. Pras, G.A. Mitchell, J.L. Michaud, D.B. Goldstein, Deficiency of asparagine synthetase causes congenital microcephaly and a progressive form of encephalopathy, Neuron 80 (2013) 429–441.

[2] S. Ben-Salem, J.G. Gleeson, A.M. Al-Shamsi, B. Islam, J. Hertecant, B.R. Ali, L. Al-Gazali, Asparagine synthetase deficiency detected by whole exome sequencing causes congenital microcephaly, epileptic encephalopathy and psychomotor delay, Metab. Brain Dis. 30 (3) (2014) 687–694.

[3] M. Alfadhel, M.T. Alrifai, D. Trujillano, H. Alshaalan, A. Al Othaim, S. Al Rasheed, H. Assiri, A.A. Alqahtani, M. Alaamery, A. Rolfs, W. Eyaid, Asparagine synthetase deficiency: new inborn errors of metabolism, JIMD Rep. 22 (2015) 11–16.

[4] N.G. Richards, M.S. Kilberg, Asparagine synthetase chemotherapy, Annu. Rev. Biochem. 75 (2006) 629–654.

[5] H. Thorvaldsdóttir, J.T. Robinson, J.P. Mesirov, Integrative Genomics Viewer (IGV): high-performance genomics data visualization and exploration, Brief. Bioinform. 14 (2013) 178–192.

[6] T.M. Larsen, S.K. Boehlein, S.M. Schuster, N.G. Richards, J.B. Thoden, H.M. Holden, I. Rayment, Three-dimensional structure of *Escherichia coli* asparagine synthetase B: a short journey from substrate to product, Biochemistry 38 (1999) 16146–16157.

[7] M. Biasini, S. Bienert, A. Waterhouse, K. Arnold, G. Studer, T. Schmidt, F. Kiefer, T.G. Cassarino, M. Bertoni, L. Bordoli, T. Schwede, SWISS-MODEL: modelling protein tertiary and quaternary structure using evolutionary information, Nucleic Acids Res. 42 (2014) W252–W258.

[8] K. Arnold, L. Bordoli, J. Kopp, T. Schwede, The SWISS-MODEL workspace: a web-based environment for protein structure homology modelling, Bioinformatics 22 (2006) 195–201.

[9] F. Kiefer, K. Arnold, M. Künzli, L. Bordoli, T. Schwede, The SWISS-MODEL repository and associated resources, Nucleic Acids Res. 37 (2009) D387–D392.

[10] N. Guex, M.C. Peitsch, T. Schwede, Automated comparative protein structure modeling with SWISS-MODEL and Swiss-PdbViewer: a historical perspective, Electrophoresis 30 (Suppl. 1) (2009) S162–S173.

[11] J.H. Priest, Prenatal chromosomal diagnosis and cell cultureChapter 5 in: M.J. Barch (Ed.), The ACT Cytogenetics Laboratory Manual, Second editionRaven Press, New York 1991, pp. 182–183.

[12] J. Shan, W. Donelan, J.N. Hayner, F. Zhang, E.E. Dudenhausen, M.S. Kilberg, MAPK signaling triggers transcriptional induction of cFOS during amino acid limitation of HepG2 cells, Biochim. Biophys. Acta 1854 (2015) 539–548.

[13] H. Chen, Y.X. Pan, E.E. Dudenhausen, M.S. Kilberg, Amino acid deprivation induces the transcription rate of the human asparagine synthetase gene through a timed program of expression and promoter binding of nutrient-responsive basic region/leucine zipper transcription factors as well as localized histone acetylation, J. Biol. Chem. 279 (2004) 50829–50839.

[14] R.G. Hutson, T. Kitoh, D.A. Moraga Amador, S. Cosic, S.M. Schuster, M.S. Kilberg, Amino acid control of asparagine synthetase: relation to asparaginase resistance in human leukemia cells, Am. J. Physiol. 272 (1997) C1691–C1699.

[15] M.N. Balasubramanian, E.A. Butterworth, M.S. Kilberg, Asparagine synthetase: regulation by cell stress and involvement in tumor biology, Am. J. Physiol. Endocrinol. Metab. 304 (2013) E789–E799.

[16] M.S. Kilberg, M. Balasubramanian, L. Fu, J. Shan, The transcription factor network associated with the amino acid response in mammalian cells, Adv. Nutr. 3 (2012) 295–306.

[17] R.A. Hawkins, R.L. O'Kane, I.A. Simpson, J.R. Vina, Structure of the blood–brain barrier and its role in the transport of amino acids, J. Nutr. 136 (2006) 218S–226S.

[18] A. Visel, C. Thaller, G. Eichele, GenePaint.org: an atlas of gene expression patterns in the mouse embryo, Nucleic Acids Res. 32 (2004) D552–D556.

[19] S.N. van der Crabben, N.M. Verhoeven-Duif, E.H. Brilstra, L. Van Maldergem, T. Coskun, E. Rubio-Gozalbo, R. Berger, T.J. de Koning, An update on serine deficiency disorders, J. Inherit. Metab. Dis. 36 (2013) 613–619.

[20] L. Hertz, The glutamate–glutamine (GABA) cycle: importance of late postnatal development and potential reciprocal interactions between biosynthesis and degradation, Front. Endocrinol. 4 (2013) 59.

[21] A. Lau, M. Tymianski, Glutamate receptors, neurotoxicity and neurodegeneration, Pflugers Arch. 460 (2010) 525–542.

[22] M. Jia, S.A. Njapo, V. Rastogi, V.S. Hedna, Taming glutamate excitotoxicity: strategic pathway modulation for neuroprotection, CNS Drugs 29 (2015) 153–162.

[23] K. Tufan, N. Oztanir, E. Ofluoglu, C. Ozogul, N. Uzum, A. Dursun, H. Pasaoglu, A. Pasaoglu, Ultrastructure protection and attenuation of lipid peroxidation after blockade of presynaptic release of glutamate by lamotrigine in experimental spinal cord injury, Neurosurg. Focus. 25 (2008) E6.

[24] M. Bodmer, M. Sulz, S. Stadlmann, A. Droll, L. Terracciano, S. Krähenbühl, Fatal liver failure in an adult patient with acute lymphoblastic leukemia following treatment with L-asparaginase, Digestion 74 (2006) 28–32.

[25] C. Al-Nawakil, L. Willems, C. Mauprivez, B. Laffy, M. Benm'rad, J. Tamburini, H. Fontaine, P. Sogni, B. Terris, D. Bouscary, L. Moachon, Successful treatment of L-asparaginase-induced severe acute hepatotoxicity using mitochondrial cofactors, Leuk. Lymphoma 55 (2014) 1670–1674.

[26] K. Danhauser, J.A. Smeitink, P. Freisinger, W. Sperl, H. Sabir, B. Hadzik, E. Mayatepek, E. Morava, F. Distelmaier, Treatment options for lactic acidosis and metabolic crisis in children with mitochondrial disease, J. Inherit. Metab. Dis. 38 (3) (2015) 467–475.

[27] A. Shrivastava, A.A. Khan, M. Khurshid, M.A. Kalam, S.K. Jain, P.K. Singhal, Recent developments in L-asparaginase discovery and its potential as anticancer agent, Crit. Rev. Oncol. Hematol. (2015).

[28] P. Curatolo, Mechanistic target of rapamycin (mTOR) in tuberous sclerosis complex-associated epilepsy, Pediatr. Neurol. 52 (2015) 281–289.

Web References

[29] CADD http://cadd.gs.washington.edu/ EXAC http://exac.broadinstitute.org; dbSNP http://www.ncbi.nlm.nih.gov/SNP; EVS http://evs.gs.washington.edu/EVS/; 1000 Genomes http://www.1000genomes.org; PROVEAN http://provean.jcvi.org.